# Length-dependent Conductance of conjugated molecular junctions


## Yizhi Wu

**S1951319**



## Abstract

Molecular junction is a promising candidate for devices nowadays, especially the conjugated molecule with much higher conductance compared to sigma bond alkanes. The decay constant β, which describes the length-dependent conductance, is one of the most important parameters in molecular junctions. To investigate the decay constant, we introduce the exponential dependence first, and then explain by theory. After the comparison of β values of conjugated systems and sigma bond compounds, we mainly focus various aspects that can affect the decay constant. The transition from tunneling to hopping is discussed in details, with several series of samples. Other aspects, such as anchor groups, twisted angles and conjugated limitations are also included.



**Key word**: conjugated, molecular length, decay constant, anchor group, tunneling, hopping, twisted angle.


## Introduction

As predicted by Gordon E. Moore in 1965, the density of transistors on integrated circuits increases in time, which requires devices in nanometers. In the past decades, molecular electronics has been investigated and proposed to be a candidate for modern devices. Molecular electronics with various and unique properties are now an alternative to conventional silicon devices, or complementary to the silicon-based microelectronics [1]. Molecules can be synthesized with desired properties properly, which performs as one of the most promising advantages in the electronic industry. Molecules possess light-weight flexibility and versatility, even optical and magnetic properties, which may be impossible for traditional devices to achieve. At the mean time, organic molecules are not competitive with silicon-based materials in operation speed, reliability, stability, power consumption, lifetime and et al. Both the advantages and shortcomings of molecular devices are attractive to investigate and improve.

Molecular conductance, the main basic feature of devices, however can not be measured accurately, varying up to 8 orders of magnitude. Various aspects affect the conductance of molecular devices in large extent, such as anchor groups, testbeds, and configuration of electrodes. To reduce these fluctuations, a large number of experiments are required to obtain reliable results of molecular conductivity from statistical analysis. Because of experimental difficulties, the available data reporting systematic analyses of such system is relatively scarce. [2] However, an exponential decrease of conductance versus increasing molecule length have been observed in both alkane(di)thiols and conjugated molecules, which is explained mainly by tunneling mechanism as discussed below.

# 1. Exponential dependence

In general, the exponential dependence of the current density with increasing molecular length is described as

$$J \propto e^{-\beta \cdot d} \quad [3, 4, 5, 6, 7]$$

Where J is the current density, beta is the decay constant in angstrom, and d is the length of the molecule. The current density can also be substituted by the conductance per molecule, which is the current measured directly for break junction measurement. For self-assembled monolayers(SAM), assumption is applied that the grafting density is maximum on Au(111), i.e. $4.6 \times 10^{7} m^{-2}$ [Fig1], [8].

Then conductance per molecule is the current density divided by the number of molecules per area. (In practice, the length of molecule is replaced by the distance between two electrodes.) β, the decay constant, also named tunneling attenuation factor, would be discussed through out this paper. In general, Beta depends on the nature of bonding in the molecular backbone.

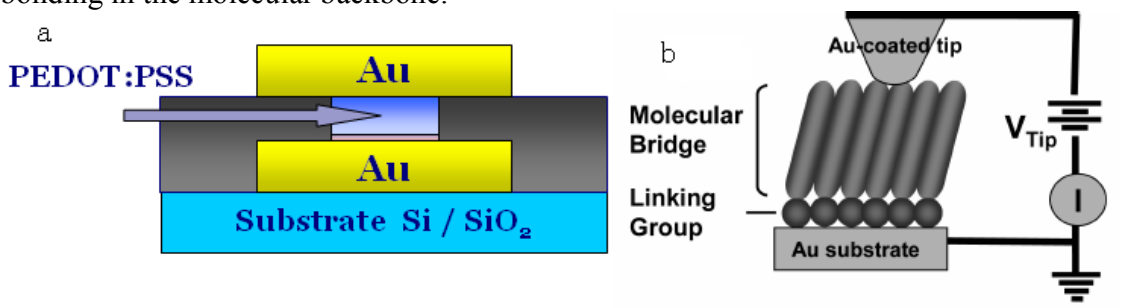


**Fig. 1** a) SAM fabricated as a sandwich in devices. SAM is deposited on gold bottom contact first, and covered by "organic metal" PEDOT:PSS and top contact. The grafting density of SAM is assumed as maximum on Au(111). b) Metal-molecule-metal junction with conducting probe atomic microscope (CP-AFM). A tip coated with gold performs as top contact to conjugated-SAM. [9]

# 2. Decay constant of alkane(di)thiols

Before discussing the β phenomena of conjugated molecules, we would show the summary of the beta data of alkane(di)thiols from Hylke B. Akkerman firstly.

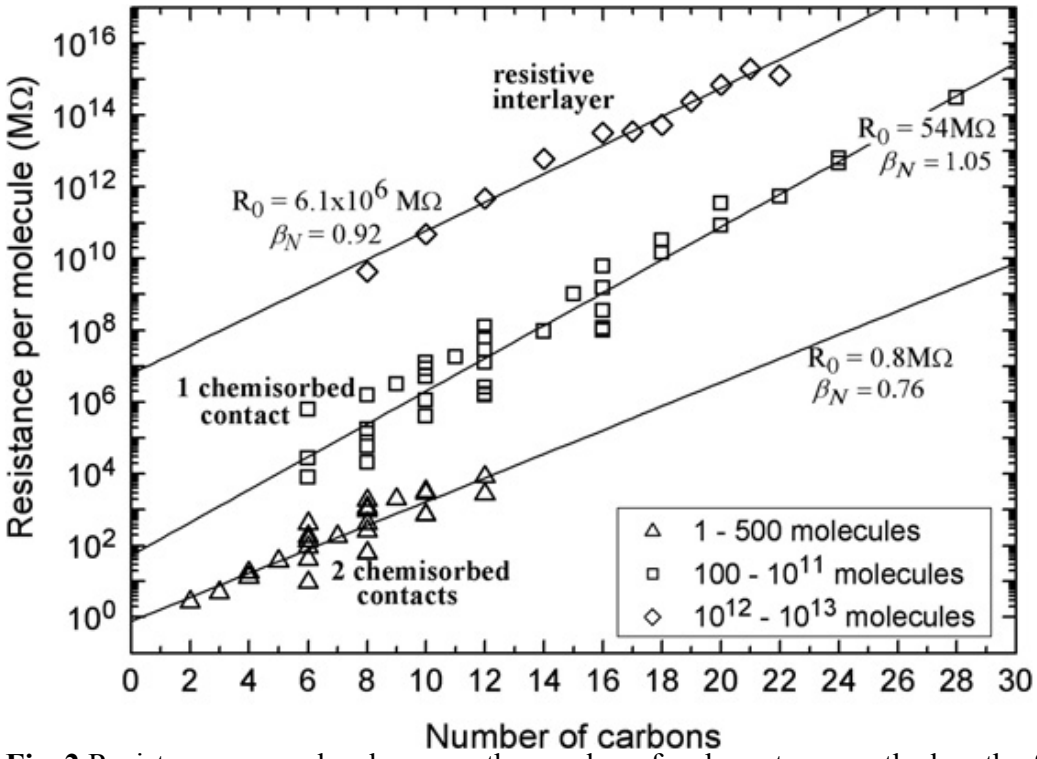


**Fig. 2** Resistance per molecule versus the number of carbon atoms, or the length of molecule is shown. The three regimes demonstrate that the method of making contact is a critical factor for the resistance, which affect the values of resistance in orders of magnitudes. $R_0$ is the contact resistance at the intercept, and $\beta_N$ is the decay factor for each series respectively. [10]

Several conclusions can be established as follows (1) The types of testbeds measured are not the critical parameters compared to other aspects; (2) The resistance per molecule can be divided by three regimes, low, medium and high resistance groups. Alkanedithiols, which contacts with electrodes at both ends by chemisorbed contacts, locate within the low resistance group, while alkanmonothiols within the medium group. Such separation implies that chemical bonding between plays a significant role in conductance. Chemisorbed contacts reduce the energy barriers between two electrodes effectively in tunneling mechanism. (3) The decay constant beta from the three groups is similar and irrelevant with the number of molecules measured, with average value of 0.92±0.19 per angstrom.

# 3. Tunneling theory

In tunneling transport theory, molecules between two electrodes are treated as energy barriers. The Simmons model, the representative quantum mechanical model for the tunneling mechanism, describes the tunneling current as follows: [11]

$$I = \frac{Ae}{4\pi^2\hbar d^2}\left\{\left(\phi - \frac{eV}{2}\right)\exp\left(-\frac{2d\sqrt{2m}}{\hbar}\sqrt{\phi - \frac{eV}{2}}\right) - \left(\phi + \frac{eV}{2}\right)\exp\left(-\frac{2d\sqrt{2m}}{\hbar}\sqrt{\phi + \frac{eV}{2}}\right)\right\} \quad \text{(eq.1)}$$

Where A is the junction area, d is the molecular length, m is the electron effective mass, φ is the barrier height, and e is the electronic charge. At low bias, the equation could be expressed approximately by

$$I \propto V \exp\left(-\frac{2d\sqrt{2m\phi}}{\hbar}\right) \quad \text{(eq.2)}$$

Hereby, in this model, beta is given by

$$\beta = \frac{2\sqrt{2m\phi}}{\hbar} \quad \text{(eq.3)}$$

The barrier height corresponds to the difference of energy level between Fermi Level of gold electrodes and highest occupied molecular orbital (HOMO), leading to different currents at identical molecular length. While the thickness of the barriers corresponding to molecular length, has an exponential relationship with current density, as shown in eq.3. All the conclusions above agree with the tunneling transition theory.

# 4. Decay constant for conjugated molecules

The experiment results of the conductance of conjugated molecules show the decay constant of conjugated molecules, in a range of 0.04-0.3 per angstrom is much lower than that of alkenedithiols. Such phenomena are very important in practical and theoretical reasons. The low decay constant implies a totally different transition mode compared to alkanedithiols, and it also shows that electrons transport could occur through out many molecules. As said by other researchers [12, 13], active molecular junctions are related to typical tunneling length in a large extent, which needs a low decay constant β. Experimental data of decay constant lower than 0.1 per angstrom are observed, which is difficult to explain by theory. The decay constant of alkenes series is supposed to be consistent with tunneling mechanism with superexchange coupling. Because the molecular orbitals are present, the decay constant is lower than in vacuum. The lower β values, less than 0.2 per angstrom, are not consistent with tunneling mechanism. This phenomenon implies a new electron transition mechanism, which is called “hopping” and will be explained in details latter.

# 5. Theoretical results of tunneling decay factor

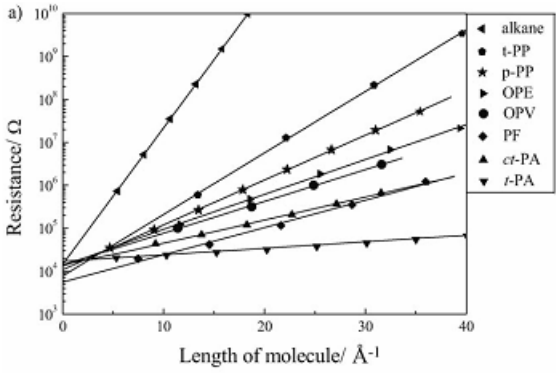


b)

| | HOMO | LUMO |
|---|---|---|
| *t*-PA | | |
| *ct*-PA | | |

**Fig. 3** a) Resistance versus molecular length in MMM junctions. b) Frontier Molecular orbital [14]

As shown in Fig 3, All resistances of molecular junctions increases with molecular length exponentially, as given by equation

$$R = R_0 \exp(\beta d) \quad \text{(eq. 4)}$$

By fitting the lines prefactors $R_0$ and tunneling decay constant β are obtained as listed in Table 1.

The saturated hydrocarbon backbones lead to a largest β value (i.e. 0.73 per angstrom), very close to that of theoretical results by Kaun and Guo.[15].

Table 2 presents the decay factor β, obtained by either experiment or theoretical calculation. Alkanes are not good candidate for modern devices because of the high resistance, while conjugated molecules can perform well in molecular junctions. In this table, we can also find that β value of the conjugated molecules also varies in a certain extent.

**Table 1.** Attenuation factor ($\beta$), contact resistance ($R_0$), and energy gap $(E_g)_\infty$ of several gold/molecule/gold junctions.

| | alkane | t-PP | p-PP | OPE | OPV | PF | *ct*-PA | *t*-PA |
|---|---|---|---|---|---|---|---|---|
| $\beta$ [Å$^{-1}$] | 0.73 | 0.33 | 0.24 | 0.19 | 0.17 | 0.16 | 0.13 | 0.036 |
| $R_0$ [kΩ] | 7.3 | 3.9 | 5.5 | 6.6 | 7.0 | 2.5 | 7.1 | 8.2 |
| $(E_g)_\infty$ [eV] | – | 2.33 | 1.83 | 1.56 | 1.24 | 1.17 | 0.85 | 0.47 |

**Table 2.** Comparison of electron-tunneling attenuation factors[a] measured by using various methods.

| Method | $\beta$ value [Å$^{-1}$] | Method | $\beta$ value [Å$^{-1}$] |
|---|---|---|---|
| **Alkane** | | molecule/nanoparticle bridge technique | 0.76 ± 0.05[28] |
| electrochemical | 0.85[2] | Ag–SAM//SAM–Hg junction | 0.87 ± 0.10[31] |
| electrochemical | 1.0[3] | metal-capped nanopores | 0.79 ± 0.10[81] |
| electrochemical | 0.91, 1.31[5] | DFT/NEGF | 0.69, 0.66[26] |
| C-AFM | 0.63 ± 0.10[10] | DFT/NEGF | 0.74[61] |
| C-AFM | 0.86 ± 0.10[11] | DFT/NEGF | 0.97[65] |
| C-AFM | 1.48[12] | ab initio | ≈ 0.5–0.9[82] |
| C-AFM | 0.94 ± 0.06[13] | DFT | 0.70[83] |
| C-AFM | 1.13[14] | **Polyphenyl** | |
| C-AFM | 1.10[15] | AC voltammetry | 0.36[4] |
| C-AFM | 0.88[16] | Ag–SAM/SAM–Hg junction | 0.61 ± 0.10[31] |
| STM | 0.41 ± 0.05[7] | C-AFM | 0.35–0.50[9] |
| STM break junction | 0.78 ± 0.10[20] | C-AFM | 0.42 ± 0.07[13] |
| STM break junction | 0.84[21] | DFT/Green function | 0.16 (planar) 0.26 (twisted)[59] |
| STM break junction | 0.79, 0.77[23] | DFT/NEGF | 0.40 (planar)[60] 0.51 (twisted) |
| STM break junction | 0.75, 0.73, 0.35[26] | **Oligoacene** | |
| SPM | 1.37 ± 0.03[80] | C-AFM | 0.51[1] |

[a] Some attenuation-factor values were converted to Å$^{-1}$ (from the unit "per methylene"). The unit length of the alkane chain is 1.28 Å.[26]

# 6. Energy gap Dependence

The behavior of electron transport is determined mainly by the intrinsic properties of molecular junctions, including the conformation, the band gap and molecular length. The

band gap ($E_g$), also named energy gap or HOMO-LUMO gap, is a critical parameter of the conductance of molecular junctions, because of the relationship with energy barriers which electrons should break through under external fields in tunneling models.

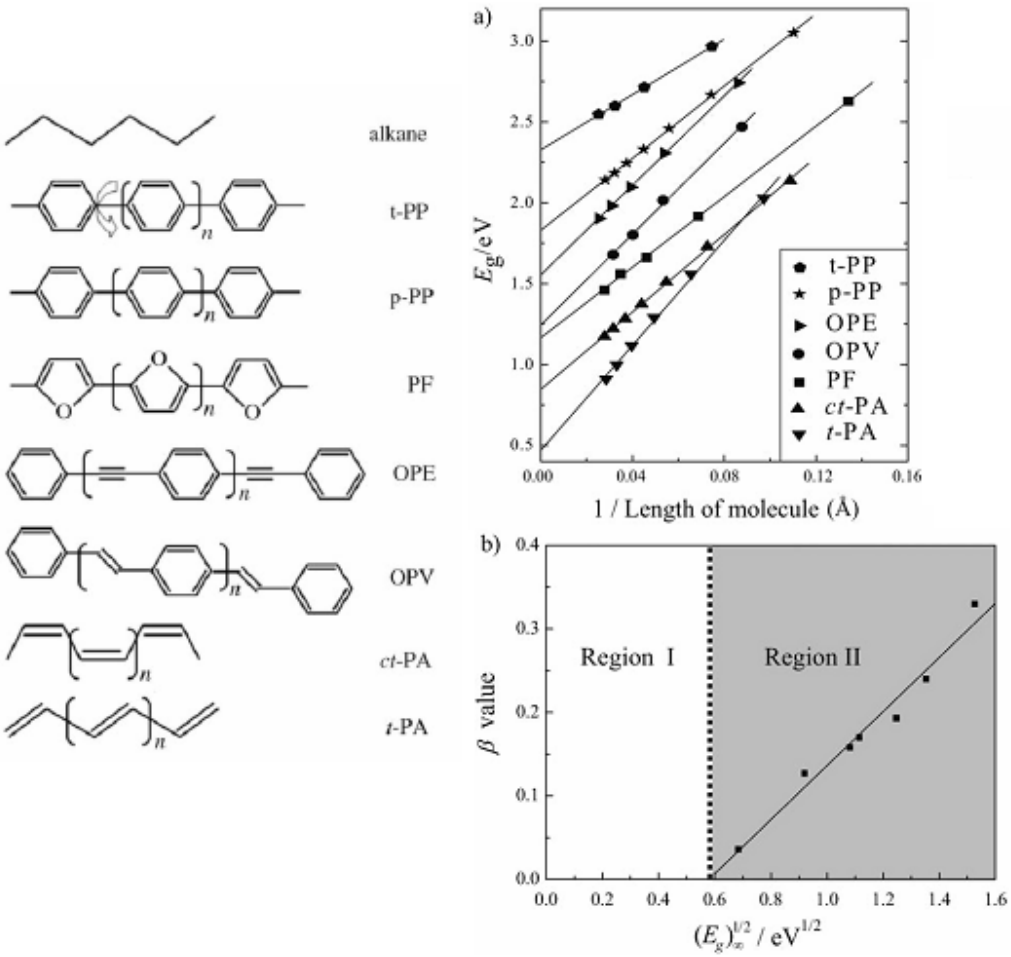


**Fig. 4** chemical structures of molecules studied here. a) linear dependence of band gap versus reciprocal molecular length in series. b) β as a function of conjugated molecules in series. $(Eg)_0$ is the energy band gap at infinite chain length.[14]

Figure 4 a) shows the relationship between molecular length and band gap ($E_g$) in series of conjugated molecules. Band gaps increase linearly in all series with increasing reciprocal chain length (decreasing molecular length in real space). It is also obvious that the band gaps reach non-zero value at 0 chain length, which is infinite molecular length in real space.

In the most widely used Simmons model, which describes the current as electrons traveling through barriers, the behavior of the current density at low bias is expressed approximately by

$$I = \frac{e^2 AV}{h^2 d}(2m\varphi)^{1/2} \exp\left[\frac{-4\pi d}{h}(2m\varphi)^{1/2}\right] \text{(eq.5)}$$

Where φ is the effective barrier height, A is the contact area, V is the bias voltage, d is the width of barrier, m is the electron mass, e is the electron charge, h is the Plank constant.

The relationship between transmission barrier φ and energy gap $(Eg)_0$ can be obtained from the linear dependence at Fig 4 b).

$$\beta = -0.19 + 0.32(E_g)_{\infty}^{1/2} \quad \text{(eq. 6)}$$

A strong relationship between decay constant and energy gap is clear as shown here. The decay constant increased with the energy gap in the order of: t-PA<ct-PA<PF<OPV<OPE<p-PP<t-PP. By compared with the energy gap, the decay constant of a certain series can be predicted from the Figure 4.

Organic molecules perform a different behavior in electron transmission from that in crystalline wires. The band gap of most organic molecules, even conjugated molecules is larger than 0.35eV, which means that the β value is nonzero. This phenomenon matches the Simmons tunneling theory. As molecular length increases, the positive β value indicates the decreased conductance, if the Fermi level of the electrodes lies between the HOMO-LUMO of the molecules. However, if the band gap is small enough, the β value would be zero, which means that the conductance would be constant and independent with molecular length. In this regime, the mechanism of electron transmission changes from tunneling model to hopping model. In hopping model, the conductance of molecular junction is no longer sensitive to molecular length, which is a promising feature of molecular devices, similar to superconductor. Conjugated molecules are divided into two regimes as shown in Fix 4 b). In regime II, molecules behave as
Twist angle normal devices, while below the threshold they perform promising properties, like superconductors. This is useful for design of molecular junction in the future.

# 7. Tunneling to hopping

# 7.1 ONI

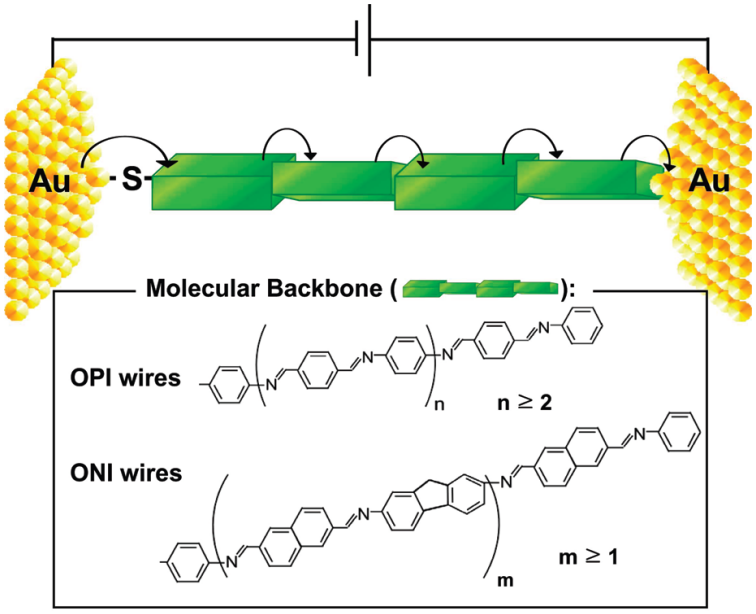


**Fig. 5** schematic cartoon of hopping mechanism in molecular junctions and structures of OPI and ONI wires. [16]

In Fig 5, hopping mechanism is depicted. The cured arrows present that electrons hop from one local site to the next site. For long molecules, tunneling mechanism is suppressed because the thickness of barrier is too large that electrons can not transmit from one of the electrodes to anther one directly. In hopping mechanism, electrons transport in series of discrete steps, including injection of the charge from one electrode, field-induced hopping along the chain of conjugated system, and exporting the charge to the other electrode.

Nowadays, most conjugated molecular junctions are short enough that the main electron transport mechanism is direct tunneling. In other words, electrons transport under external electric field from one electrode to the other. The efficiency of such mechanism, such as conductance versus molecular length, depends on the structure of the molecular backbone. There are still other aspects that could affect the conductance of molecular junctions, such as the symmetry of contact, electronic structure, and the interactions among molecules. In the regime of hopping conduction, where the length of molecules is long enough, the tunneling transmission is forbidden. Instead, the electrons should be injected from one electrode to the molecules and then move along the backbone of molecules by the external electric field until to the other electrode. Hopping mechanism is a important charge conduction mechanism in self-assembled monolayer device of conjugated molecules. Such hopping mechanism is worth to be understood better because it could be utilized in the application of organic solar cells, light emitting diodes and so on.

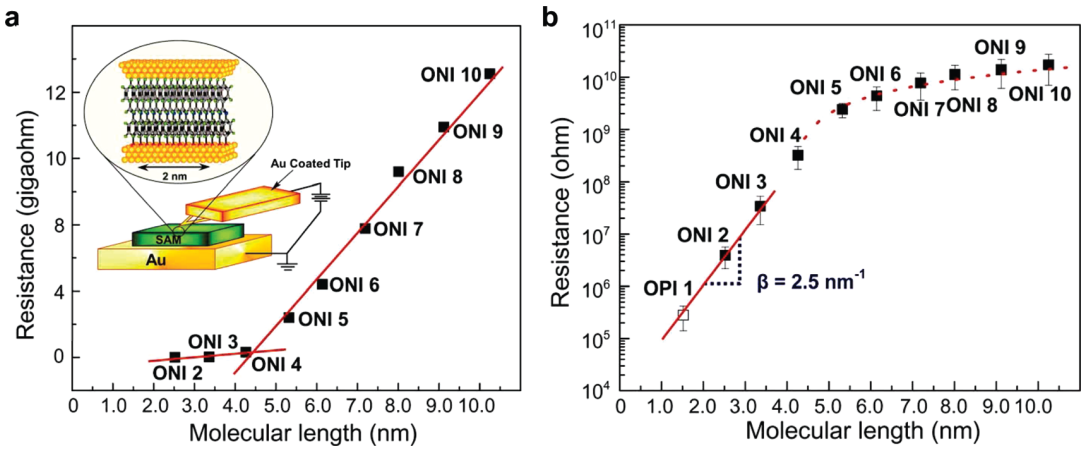


**Fig. 6** Experiment result of molecular junctions by probe atomic force microscopy. (a) A curve of resistance versus molecular length in the gold-molecule-gold junction. The resistance is an average value under different bias, from -0.1V to 0.1V. The straight lines are the linear fits of the data. The gold-coated tip contacted the self-assembled monolayer of ONI. (b) A logarithm plot of resistance versus molecular length. Resistance was measured from -0.1V to 0.1V bias. [16]

As shown in Fig 6, CP-AFM is used to measure the conductance of ONI junctions, within a small bias range ±0.1V. When molecular length is less than 4nm, corresponding to ONI 4, the normal tunneling mechanism prevails. For longer molecular length (ONI4-ONI-10), hopping mechanism becomes dominant. In this regime, the length-dependent resistance changes. In Fig 6 b) the dependence of resistance versus molecular length is weaker, which matches our theoretical explanations, because the slope is lower in the regime of long molecular length. The relationship between conductance and molecular length is still affected by intermolecular interactions. Landau et al. applied a theoretical approximation to find the effect of intermolecular interactions in conjugated molecular junctions. [17] They found that the conductance per molecule becomes larger or smaller in an adlayer, which depends on the metal-molecule coupling (alignment of Fermi level in the junction and broadening of energy levels).

The semilog curve of resistance versus molecular length in Fig 6 b) for short molecules reveal that resistance increase with the length exponentially. The decay factor β obtained from the short range is 0.25 per angstrom.

## 7.2 OPI

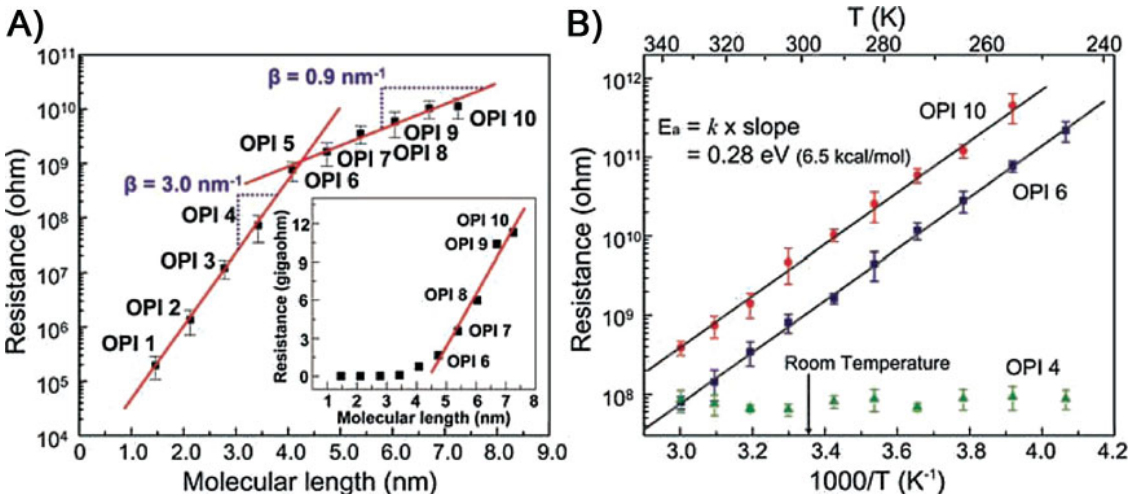


**Fig. 7** Experiment result of OPI junctions by probe atomic force microscopy. (a) A curve of resistance versus molecular length in the gold-molecule-gold junction. The straight lines are the linear fits of the data. (b) A logarithm plot of resistance versus temperature. [18]

From Fig 7, the change of transmission mechanism from tunneling to hopping is observed obviously. For short molecules (<3nm), the exponential dependence of current density versus molecular length results from electrode/molecule/electrode direct transition, namely tunneling. However, for longer molecule (>4nm), both theory and experiment on soluble donor-acceptor (DBA) systems indicate the transport mechanism changes from tunneling to hopping by the evidence of changes of the decay constant, from 0.3 for short molecules to 0.09 for longer ones.

A similar series of conjugated molecules was applied to make a junctions and similar results were obtained. As show in fig 7, oligo(p-phenylene ethynylene)s (OPE) and their derivates were deposited as self-assembled monolayer and conductance was measured.

## 7.3 OPE

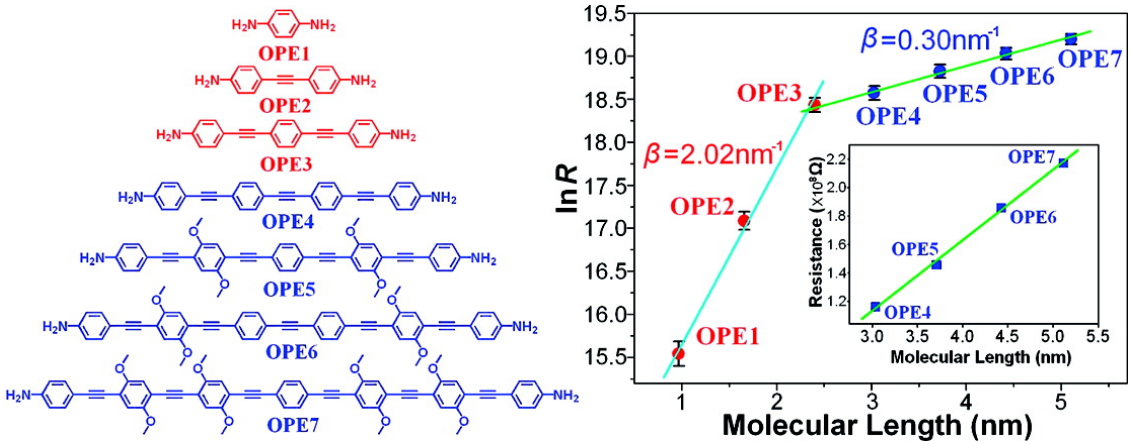

**Fig. 8** a) molecular structures of series of amine-terminated OPE in study, b) experiment result of OPE junctions by probe atomic force microscopy. A curve of resistance versus molecular length in the gold-molecule-gold junction. The straight lines are the linear fits of the data. [11]

Seven OPE molecules have been fabricated into molecular devices. An ordered self-assembled monolayer forms upon a metal substrate, which is an essential requirement of current-voltage measurement. Therefore, all the ordered and condensed monolayer should be detected by X-ray photoelectron spectroscopy before I-V measurement, to make sure that monolayer has formed.

| molecule | length (nm) | film thickness (nm) | single molecular resistance (MΩ) | $I \propto V^{\beta}$ | $I \propto V^{\beta}$ | $V_{trans}$ (V) | $V_{1/2}$ (V) |
|---|---|---|---|---|---|---|---|
| OPE1 | 0.98 | 0.49 | 5.623 ± 0.752 | 1.11 | | 0.59 | |
| OPE2 | 1.67 | 0.99 | 23.32 ± 2.47 | 1.13 | | 0.64 | |
| OPE3 | 2.41 | 1.45 | 101.0 ± 7.00 | 1.09 | | 0.65 | |
| OPE4 | 3.04 | 1.82 | 116.3 ± 8.50 | 1.15 | 2.11 | 1.14 | 0.49 |
| OPE5 | 3.73 | 2.08 | 149.9 ± 11.7 | 1.02 | 2.11 | 1.23 | 0.53 |
| OPE6 | 4.43 | 2.38 | 184.7 ± 13.7 | 1.10 | 2.13 | 1.12 | 0.52 |
| OPE7 | 5.11 | 2.65 | 217.3 ± 17.0 | 1.04 | 2.18 | 1.17 | 0.51 |

Table 3 Main parameters and experiment results of OPE molecules and their self-assembled monolayer [11]

From table 3, we can see that film thickness increases with molecular length, for the reason that the film is formed by molecular self-assemble monolayer, which means that the film thickness is proportional to molecular length. Moreover, single molecular resistance increases exponentially with increasing thickness.

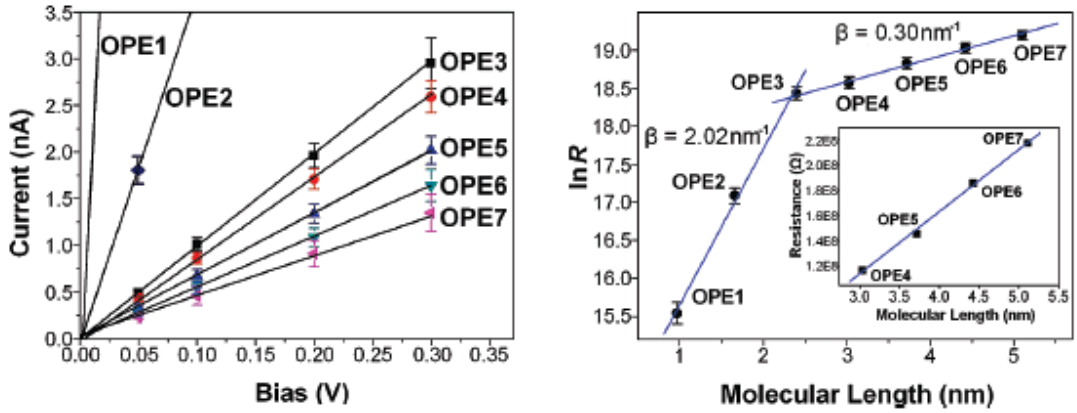


**Fig. 9** a) Current versus bias characteristics of seven OPE molecules. The slope of each OPE is nearly constant, from which the absolute resistance can be calculated. b) Logarithm of single OPE molecular resistance versus molecular length in a metal-molecule-metal junction. [11]

From Fig 9 a), we can see that the relationship between current and bias is linear for each OPE molecule, which means the resistance per molecule is constant at low bias in this case. As for Fig 9 b), the resistance per molecule can be divided into two regimes as the same with OPI and ONI discussed before. The change of transition mechanism occurs at OPE3, corresponding to about 2.5 nm, which is a bit different from OPI and ONI. In my

opinion, the reason for the difference is that carbon- bone structure of OPE is more linear compared to OPI and ONI. Thus, conjugated systems can communicated with each other along the same molecule much better. Hopping mechanism occurs at shorter length than before.

| Molecule Series | Decay constant in tunneling / $\dot{A}$ | Decay constant in hopping / $\dot{A}$ | Threshold | Molecular length of Threshold |
|---|---|---|---|---|
| ONI | 0.25 | 0.06 | ONI4 | 4.4nm |
| OPI | 0.30 | 0.09 | OPI5 | 4.0nm |
| OPE | 0.20 | 0.03 | ONI3 | 2.5nm |

Table 4 Comparison of ONI/OPI/OPE in transition from tunneling to hopping mechanism.

From table 4, a couples of conclusions can be drawn: 1) The decay constant of conjugated systems, about 0.2-0.4 per angstrom, is much lower than alkandithiols series, implying the decrease of energy barriers for conjugated junctions. 2) The ratios of decay constant between tunneling and hopping mechanism is about 4 times to 6 times, which is a strong evidence of a change in transition. 3) The lower decay constant implies the resistance per molecule is less dependent of molecular length. This phenomenon is consistent with the hopping mechanism, as electrons transport trough a whole molecule in a couple of steps instead of tunneling at one time. 4) The thresholds of various conjugated systems are similar and irrelevant with periods. In this case, hopping mechanism is sensitive to molecular length instead of the number of conjugated periods, which implies the size of hopping sites is irrelevant with that of conjugated periods.

In practice, it is difficult to systematically measure to the boundary between hopping and tunneling regimes, owing to the difficulty in the synthesis of long conjugated molecules in series.

## 7.4 Temperature dependence of hopping mechanism

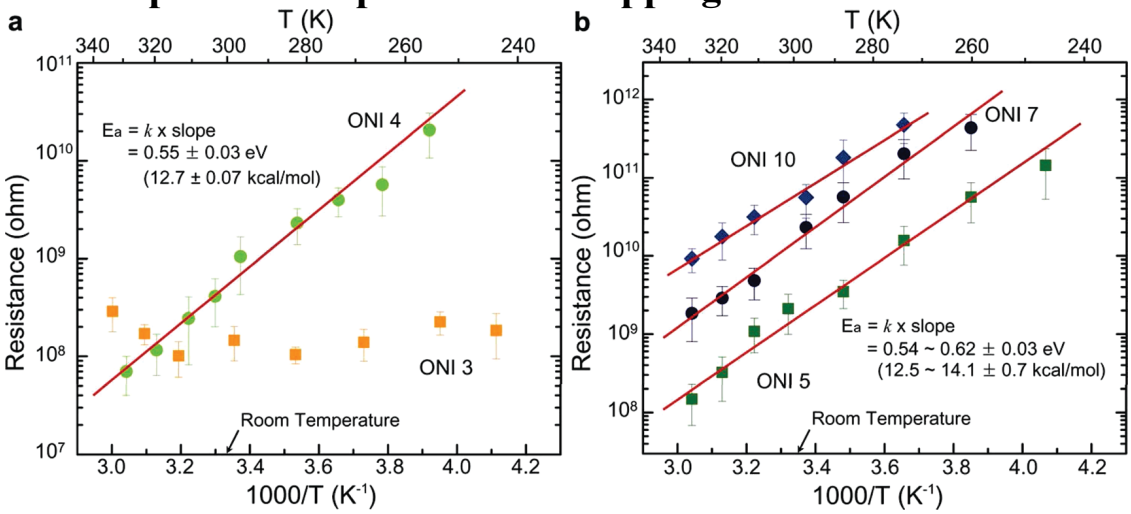


**Fig.10** The temperature depengdent resistance of ONI series.[16]

The relationship between resistance and molecular length is a strong evidence for the change of transport mechanism, but the temperature dependence is also a good method to distinguish these mechanisms. Fig.10 shows resistance of certain ONI molecules versus inverse of temperature. It is obviously that the resistance of ONI3 is independent of temperature, from 246K to 333K, which is consistent with tunneling mechanism. For the longer ONI molecules, as ONI4, ONI6, however, the resistances are strongly dependent to temperature. The linear fits show that the resistances of longer molecules are proportional to the inverse of the temperature. Such phenomenon implies that the hopping mechanism is thermal activated transmission.

Moreover, the slopes of the linear fits are almost identical to each other, which means in hopping mechanism the rate-determining steps are identical, and irrelevant to the molecular length. A similar change from tunneling to hopping mechanism is observed at OPI series. Both ONI and OPI series change the transport mechanism from tunneling to hopping at about 4 nm. A theoretical explanation of the temperature-dependent resistance is carried out by Segong Ho Choi group. In their theory, isolated and positively charged ONI junctions are under research. The charge hopping rate ($k_{et}$) is expressed by

$$k_{et} \propto \exp(-\frac{(\lambda + \Delta G^o)^2}{4\lambda k_B T}) \quad \text{(eq.7)}$$

Where $\lambda$ is the reorganization energy, $k_B$ is the Boltzmann constant and T is the temperature, $\Delta G^o$ is the thermodynamic driving force, which is considered to be the variation energy of the first approximation.

## 7.5 Quantum chemistry theory

The hopping mechanism could also be explained by quantum chemistry calculation. The charge transport is affected by molecular structure, the energy band gap. The HOMO and LUMO are the alignment of frontier orbitals to the Fermi level of metal electrodes. If the difference of LUMO and Fermi level is large, the transition mechanism is tunneling. When the LUMO level is closed to the Fermi level, then the hopping mechanism can occur. As shown in Fig 11, the level of LUMO in OPE series decreases with increasing number of Phenyl Rings. The LUMO level decreases significantly in the first three compounds, and after OPE4 the energy gaps are much smaller than before. This trend is consistent with the measurement results of conductance versus molecular length.

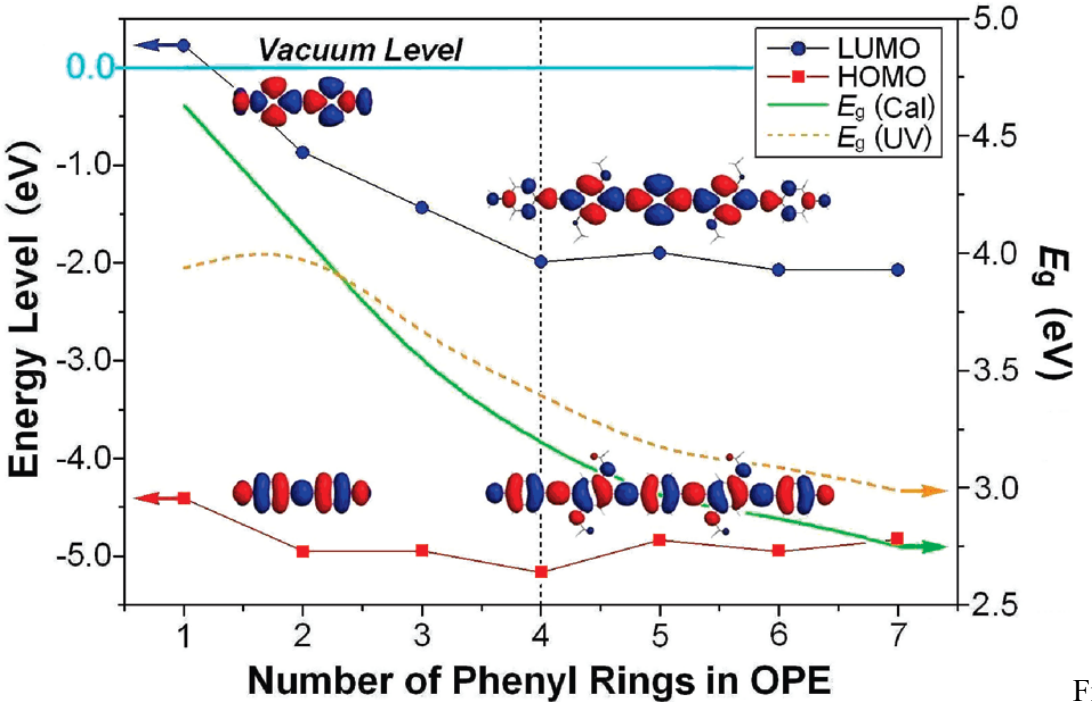


Fig **Fig.11** The alignment of HOMO, LUMO and Fermi level of OPE junctions, obtained by UV-visible spectroscopy and quantum chemistry calculation. [11]

## 8. Anchor group

Metal-molecule contacts and the electronic structure of the molecular backbone are important aspects in the conductance of metal-molecule-metal (MMM) junctions. Most experiments of molecular junction use thiol (-S) metal contact, while various anchor group, including –O, -S, -CN (isocyanide), -Se, are also studied in theory. BongSoo Kim, Jeremy, and et al, measured the conductance of series of oligoacences with increasing length based on SAMs. [fig 12]

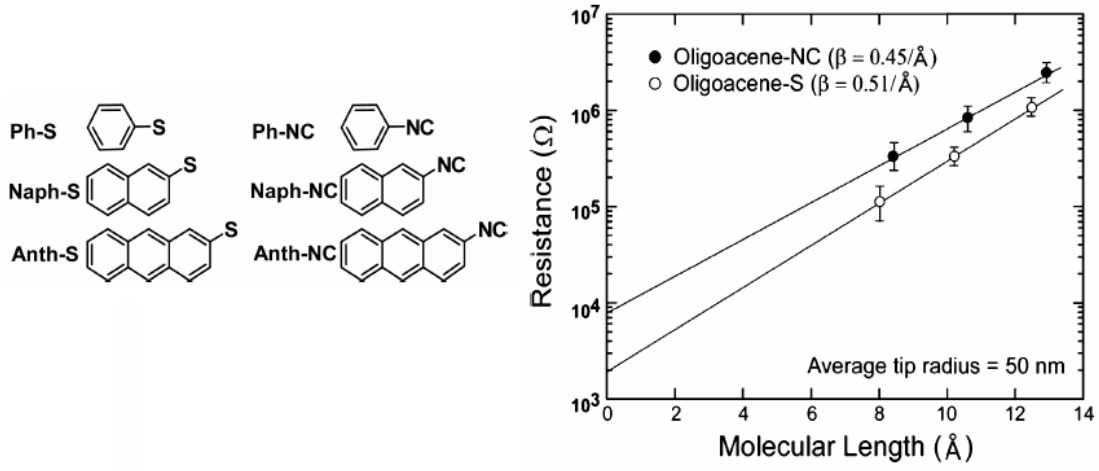

**Fig.12** Series of conjugated oligoacenes with different anchor groups (-S or -NC) and Resistance versus molecular length based on SAM devieces. Linear fits to the dates show different intercepts and slopes, corresponding to different resistances and decay Constant β [9].

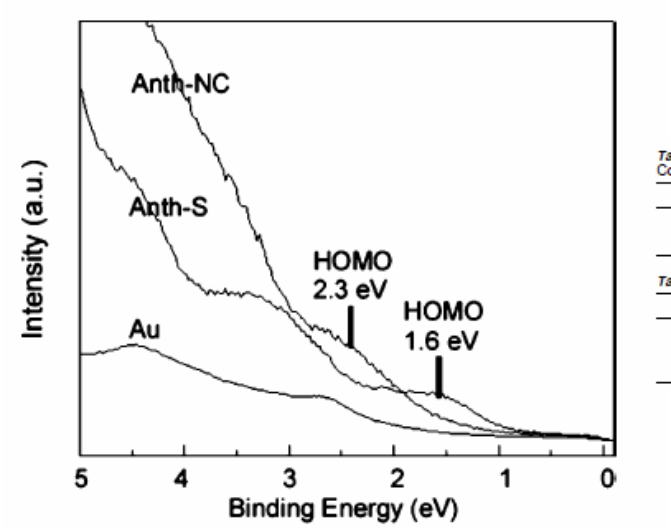


*Table 1.* Length-Dependent Tunneling Attenuation Factors ($\beta$) and Contact Resistances ($R_0$) for Each Molecular Series

| molecular series | $\beta$ (Å$^{-1}$) | $R_0$ (Ω) |
|---|---|---|
| oligoacene-S | 0.50 (±0.09) | 1.3 (±1.2) × 10$^3$ |
| oligoacene-NC | 0.49 (±0.08) | 3.6 (±1.9) × 10$^3$ |

*Table 2.* Energy Offsets ($E_{Fermi} - E_{HOMO}$) of SAMs on Au (eV)

| | $E_{Fermi} - E_{HOMO}$ | | $E_{Fermi} - E_{HOMO}$ |
|---|---|---|---|
| Ph-S | 2.0 | Ph-NC | 3.3 |
| Naph-S | 1.8 | Naph-NC | 2.8 |
| Anth-S | 1.6 | Anth-NC | 2.3 |

**Fig.13** Ultraviolet photo-electron spectrum for MMM junctions with different anchor groups Anth-S and Anth-NC and bare gold. Binding energy is referenced to $E_{fermi}$, and the intensities of the raw spectra were normalized at $E_{fermi}$. [9]

As shown in Fig 14, Au-CN contact is more resistive than Au-S.As mentioned before, the tunneling current depend on the barrier height between top and bottom contacts, which can be explained simply as the difference between the Fermi level of electrode and HOMO of molecule. From Table 2, the difference between these two levels decreases with increasing molecular length or the size of conjugated system, as expectation. The offset $E_{Fermi}$-$E_{HOMO}$ is the reason of the different contact resistance.

Because of the delocalization of HOMO for both the thiol and the isocyanide molecules across the anchor groups and conjugated systems, the change of molecular length could also affect the decay constant β. The higher the $E_{Fermi}$-$E_{HOMO}$ is, the smaller the decay constant β is. However, the difference is not so obvious; indicating the influence of anchor group towards the decay constant is not a significant factor.

# 9. Conjugated limitation

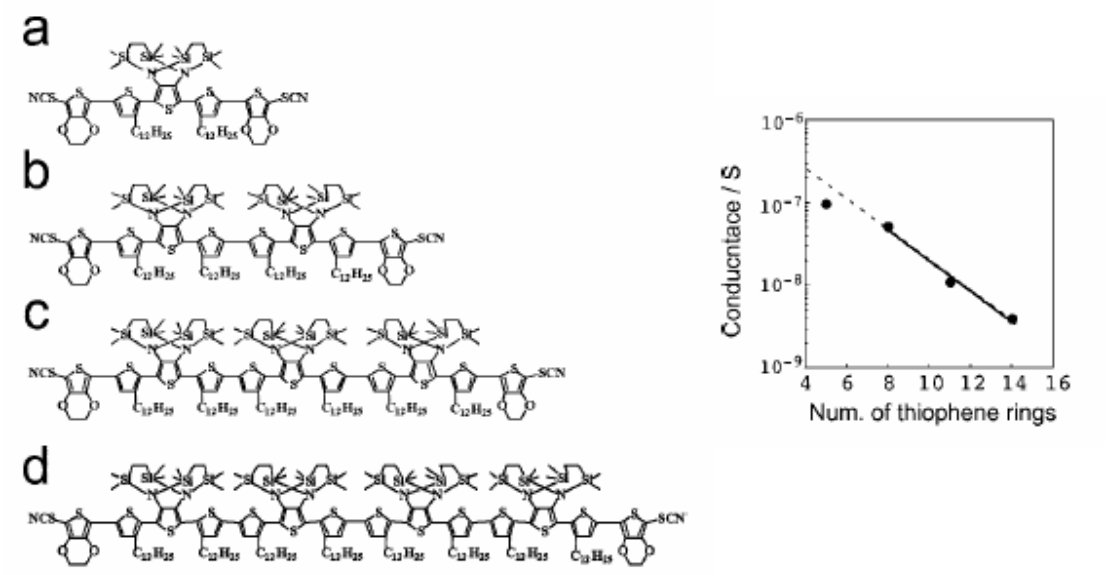


**Fig.14** structures of conjugated molecules in the study (a) 5T-di-SCN, (b) 8T-di-SCN, (c) 11T-di-SCN, (d) 14-di-SCN and linear relationship of conductance and thiophene rings. [19]

As shown is Fig 14, the conductance of this series of conjugated molecules is still has a linear relationship with molecular length, with a decay constant 0.1 per angstrom. However, there is a strange point in this figure that the conductance of 5T-di-SCN is smaller than expected. The change of the HOMO-LUMO energy gap could be the reason of this discrepancy. As we know, the energy gaps of conjugated molecules are proportional to the inverse of molecular length. In this case, the energy gap is proportional to the reciprocal number of periods. Thus, as expected, the conductance should be larger as the number of thiophene groups increases, for the band gap is supposed to be smaller. However, UV-Vis absorption spectrums were measured for all the conjugated molecules shown in Fig 14. All these molecules have absorption peaks at about 540 nm, which means the conjugation systems are confined to 5 thiophene groups. For longer molecules, because of the rotation along carbon bonds, the conjugated systems could not communicate with each other any longer. It is supposed that if molecules are stretched in break junction measurement, the conjugated system is expected to be longer with lower band gap consequently.

Electronic delocalization is limited in aromatic oligoimines because of the nonzero dihedral angle between the benzene ring and the amine bonds. The molecular wires are not flat and pi-conjugated system is broken. The band gaps in the series of ONI OPI OPE remain constant when the molecular length increases to a critical point.

# 10. Twisted angle

In conjugated junctions, molecules are composed of conjugated rings. The steric effect causes the distortion of molecules. As the molecules twist along carbon-carbon single bonds, the conjugated systems are broken. The effect of the torsion angle on properties of

molecules was discussed by Grave et al [19]. The main difference of conductance between twisted and planar structures is caused by the communication of pi electrons. In twisted molecules, the conjugated subunits are broken. Therefore, the conjugated molecules are either twisted to an optimized angle in vacuum, or planar as the strong inter-molecule interactions [20, 21, 22].

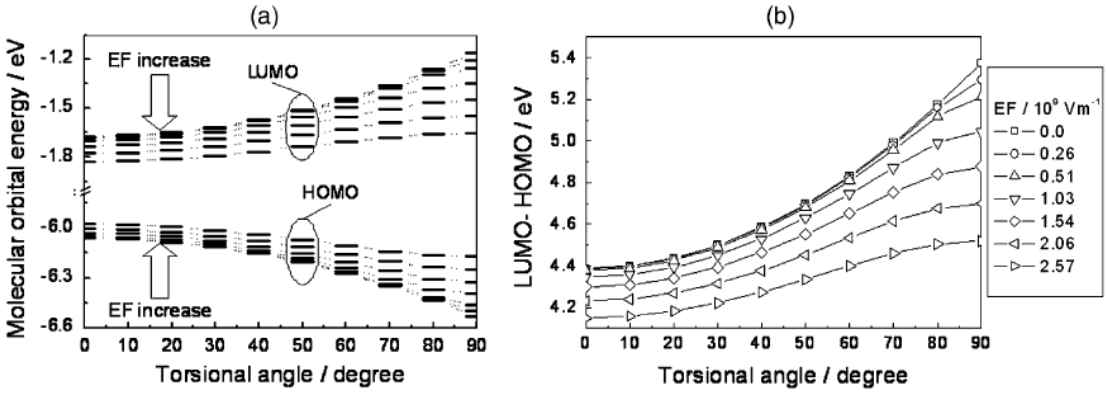


**Fig.15** The energy level of diphenylacetylene as a function of both torsion angle and external bias field [23]

As shown in Fig 15, as the torsion angle of diphenylacetylene increases, the HOMO-LUMO energy gap also increases. The breakage of conjugated systems attribute to this effect. When the applied external electric field increases, such effect is attenuated, which implies that the electric field could reduce the torsion effect.

## 11. β phenomenon of Polymer

It is a interesting discovery and promising field that the exponential length-dependent conductance is not limited in molecular junctions with two electrodes. A measurement about the conductance of conjugated polymers is carried out and the conductance is still dependent with molecular length exponentially. The structure of the conjugated polymer is shown in Fig 16, and STM measurement was carried out. When the STM tip retracts the

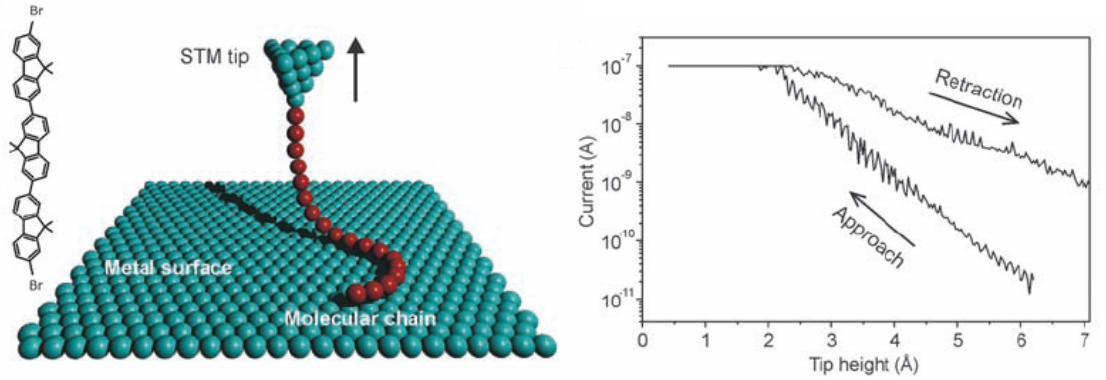

**Fig.16** Molecular structure of the polymer and scheme of STM measurement, and current versus tip height. [24]

Polymer away from the metal surface, the current decreases exponentially with increasing tip height, while when the tip approaches the metal surface, current increases exponentially again with different slope. The path-dependent current could be explained by the contact angle of polymer against surface. The contact angle varies with different path way, corresponding to different effective molecular length in junction. From this phenomenon, a conclusion can be drawn that the exponential length-dependent is an intrinsic feature of conjugated polymers, irrelevant with electrodes. The torsion angle of phenyl units are around 31.2-31.9 degree in t-PP. Because the conjugated system is broken over the whole molecule, the band gaps of twisted molecules are larger than that of planar ones, which contributes to lower conductance in junctions.

# Conclusion

In this paper, we introduce the physical characteristics of molecular junction, which is a promising candidate for modern devices. Both the advantages and shortcomings of molecular devices are attractive to investigate and improve. The exponential dependence of the current density with increasing molecular length is explained in the first place.

$$J \propto e^{-\beta \cdot d}$$

The decay constant β is defined here, which is the topic of this paper. β describes the dependence of current density versus molecular length.

To measure the conductance of molecular junctions, there are three main types of testbeds, large area molecular junctions (self-assembled monolayers), conduction probe atomic microscopic (CP-AFM ) and break junctions (BJ). The testbed is the first influence of the value of β. General speaking, conductance measured by SAM is normally larger than by BJ.

The experiment results of alkane(di)thiols are presented first, for the further comparison between conjugated molecules and alkanes. In this section, some conclusions can be drawn. 1) The testbed effect is not dominant compared to other aspects; 2) conductance of alkane(di)thiols is divided into three regimes, corresponding to the anchor groups, 3) the decay constants are similar in different regimes.

The tunneling theory is introduced to explain the electron transport mechanism. At low bias, the value of β can be expressed approximately by

$$\beta = \frac{2\sqrt{2m\phi}}{\hbar}$$

Where φ is the energy difference between Fermi level of electrodes and HOMO or LUMO level of conjugated molecules. From the expression, the decay constant is relevant with molecule orbitals.

The decay constant of conjugated molecules ranges from 0.1 to 0.4 per angstrom, which is lower by one order of magnitude than that of sigma-bond ones (1.0 per angstrom).

Such phenomenon implies that the energy band gap not only affect the absolute conductance but also the decay constant.

From theoretical calculation, the decay constant strongly depends on the energy band gap. The relationship of β and band gap is expressed by:

$$\beta = -0.19 + 0.32(E_g)_{\infty}^{1/2}$$

As band gaps increase, the dependence of conductance per molecule versus molecular length becomes more and more strong. If the band gap could be lower than a critical point, conductance would not change by molecular length by theory.

The main difference between conjugated junctions and sigma ones is that transport mechanism shift from tunneling to hopping. In hopping mechanism, electrons hop along the whole molecules by steps. In this case, the length-dependence is attenuated. A significant difference between hopping and tunneling is that conductance is a function of temperature. By comparing ONI, OPI and OPE series, I find the threshold from tunneling to hopping is almost identical, which indicates threshold mainly depends on molecular length.

Many other aspects, as anchor groups, contact symmetry, twisted angle and conjugated limitation will affect the decay constant in different ways. 1) Anchor groups change the relative positions between the Fermi-level of electrodes and HOMO-LUMO level of molecules, which affects the energy difference φ discussed before. 2) If molecules are twisted by steric hindrance, breakage of π-conjugated systems occurs. Therefore, the conductance increases, because of the increase of HOMO-LUMO gap. 3) The conjugated limitation confines the size of conjugated system, so the band gap in non-zero for conjugated molecules with infinite length. 4) The β phenomenon also appears in conjugated polymers, implying that the exponential length-dependent conductance is the intrinsic characteristic of molecular junction.

# Acknowledgement

My supervisors Hennie Valkenier and Auke J. Kronemeijer play an important role in this paper. They gave me guidance over this field and instructions about how to focus on particular topic. My mentor J.C. Hummelen helped me to choose the topic and gave me general instructions.

[1] N.J.Tao, Electron transport in molecular junctions, Nature nanotechnology, vol1 Dec 2009
[2] J.Reichert, R. Ochs, D.Bechmann, H.B.Weber, M.Mayor, H.v. Lohneysen, Phys.Rev.Lett.2002, 88,176804
[3] Akkerman HB, Blom PWN, de Leeuw DM and de Boer B (2006) Nature 411 69
[4] Suzuki M, Fujii S and Fujihira M (2006) Jpn.J.April.phys.45.2041
[5] Sakaguchi H, Hirai A, Iwata f, Sasaki A, Nagamura T, Kawata E and Nakabayashi S (2001) Appl.Phys.Lett. 79 3708
[6] Cui XD, Primak A, Zarate X, Tomfohr JK, Sanker OF, Moore AL, Moore TA, Gust D, Nagahara LA and Lindsay SM (2002) J.Phys.Chem.B 106 16801

[7] Wang W, Lee T and Reed MA (2003) Phys.Rev.B 68 035416
[8] Love JC., Estorff LA, Kriebel JK, Nuzzo RG and Whitesides GM (2005) Chem.Rev.105 1103
[9] BongSoo Kim, Jeremy M. Beebe, Yongseck Jun, X.-Y.Zhu, C. Daniel Frisbie, Am.Chem.Soc.2006, 128, 4970-4971
[10] H.B. Akkerman, B. De Boer, J.Phys.: Condens.Matter, (2008), 20, 013001
[11] Qi Lu, Ke Liu, Hongming Zhang, Zhibo Du, Xianhong Wang, and Fosong Wang (2009) Acsnano Vol3, 3861-3868
[12] G. Sedghi, K. Sawada, L.J. Esdalie, M. Hoffmann, H. L. Anderson, D.Bethell, W. Haiss, S.J. Higgins, R.J.Nichols, (2008), Am.Chem.Soc, 130, 8582
[13] R. Yamada, H, Kumazawa, T. Noutoshi, S. Tanaka, H. Tada, (2008), Nano Lerr, 8, 1237.
[14] Hongmei Liu, Nan Wang, Jianwei Zhao, Yan Guo, Xing Yin, Freddy Y.C. Boey, and Hua Zhang, (2008) ChemPhyChem, 9, 1416-1424
[15] C.C Kaun, H. Guo, Nano Lett. 2003, 3, 1521-1525
[16] Seong Ho Choi, Chad Risko, M.Carmen Ruiz Delgado, BongSoo Kim, Jean-Luc Bredas and C.Daniel Frisbie, (2010), Am.Chem.Soc, 132, 4358-4368
[17] Landau. A, Kronik. L, Nitzan. A, (2008) J.Comput.Theor.Nanosci, 5, 535-544
[18] Richard, L. McCreery, Adam Johan Bergren, (2009) Adv. Mater., 21, 1-20
[19] Ryo Yamada, Hiroaki Kumazawa, Tomoharu Noutoshi, Shoji Tanaka, Hirokazu Tada, (2008), Am.Chem.Soc
[20] T. Ishida, W. Mizutani, Y. Aya, H. Tokumoto, (2002), J. Phys.Chem. B, 106, 5886-5892
[21] D.J. Wold, R. Haag, M.A. Rampi, (2002), C.D. Frisbe, J.Phys.Chem. B, 106, 2813-2816
[22] X.Y. Xiao, B.Q. Xu, N.J. Tao, (2004), Nano Lett, 4, 267-271
[23] Yanwei Li, Jianwei Zhao, Xing Yin, Hongmei Liu, Geping Yin, (2007) Phys.Chem, 9, 1186-1193
[24] Leif Lafferentz, Francisco Ample, Hao Yu, Stefan Hecht, Christian Joachim, Leonhard Grill, (2009), Science, 323